IJIE

INTERNATIONAL JOURNAL OF INTEGRATED ENGINEERING
ISSN: 2229-838X e-ISSN: 2600-7916

Vol. 18 No. 5 (2026) 282-298
https://publisher.uthm.edu.my/ojs/index.php/ijie

Graphene-Enhanced SCMs: Impact on Cement Paste Properties

Khairul Nazhan Khairul Izwan[1], Nazirah Mohd Apandi[1]*, Warid Wazien Ahmad Zailani[1], Alia Sofea Shamsol[1], Hazlin Hamdan[2]

[1] *Faculty of Civil Engineering,*
Universiti Teknologi MARA, 40450 Shah Alam, Selangor, MALAYSIA
[2] *Denka Construction Solutions Malaysia Sdn Bhd, 40200 Shah Alam, Selangor, MALAYSIA*

*Corresponding Author: nazirahapandi@uitm.edu.my
DOI: https://doi.org/10.30880/ijie.2026.18.05.025

Article Info

Received: 17 July 2025
Accepted: 10 August 2026
Available online: 20 October 2026

Keywords

Supplementary cementitious material, graphene, physical properties, mechanical properties, durability properties, cement paste

Abstract

This study investigates the influence of supplementary cementitious materials (SCMs), specifically slag and fly ash, in conjunction with graphene nanomaterial, on the properties of cement paste. Graphene, a two-dimensional carbon allotrope with extraordinary properties, has emerged as a promising nanomaterial to enhance the performance of various materials, including cement-based composites. This study delves into the synergistic effects of graphene and supplementary cementitious materials (SCMs), specifically slag and fly ash, on the properties of cement paste. The integration of graphene into the cement matrix was found to significantly improve the stiffness and durability properties of the cement paste. Not only that, but the mechanical properties, such as compressive strength, flexural strength, and tensile strength, were also found to be enhanced with the inclusion of graphene in the cement matrix. The results demonstrated that incorporating SCMs and graphene significantly improved the mechanical properties, reduced porosity, and enhanced the durability of cement paste. The synergistic effect of SCMs and graphene was found to be particularly beneficial in improving the overall performance of cement paste. The unique properties of graphene, including its high surface area, excellent electrical conductivity, and mechanical strength, contribute to its effectiveness in improving the overall performance of cement-based materials. This study highlights the potential of graphene as a sustainable and high-performance additive for future generations of cement matrix studies.

1. Introduction

Until today, ordinary Portland cement (OPC) has been widely used as a major construction material in civil engineering. It has been reported that global cement production has reached approximately 3.6 billion tonnes as mankind's urbanisation continues to drive development in construction and infrastructure, especially in fast-developing countries such as Canada, India, and the United Kingdom [1]. Cement has been widely used in civil engineering for several reasons, including low cost, ease of use, abundant raw materials, and high compressive strength [2]. Nevertheless, concrete faces a common issue of brittleness, which directly leads to poor resistance to crack formation and strain capacity, and even lowers the stiffness of the concrete itself. This will lead to major

This is an open access article under the CC BY-NC-SA 4.0 license.

problems in the future, as it may reduce durability and increase maintenance costs [3]. Further into the hardening stage of cementitious composites, voids and cracks more readily appear on the surface of the structure due to the low tensile strength of cement paste and its low fracture toughness [4]. Thus, this indirectly leads to a restoration process for these structures as mitigation against further cracking, such as steel straps, which tend to ensure post-tensioning pressure on the surface of the concrete [5], [6].

Hence, many attempts have been made to directly overcome this issue by introducing fibre-based composite materials. Fibre Reinforced Concrete has been proposed because it can provide significant tensile strength and toughness. It is worth noting that the use of reinforcement may reduce air voids in the matrix during the material development phase. Nevertheless, it also reduces compressive strength, as the addition of fibres tends to introduce air voids in the matrix during casting [7]. Not only that, but FRC also indicated that the fibre fails to prevent crack initiation at the nanoscale, which indirectly leads to even lower mechanical performance. This allows the path of nanotechnology advancement study to align with this research as it provides four major mechanisms: (i) Serving as a filler material; (ii) Boosting pozzolanic reactivity; (iii) Regulating cement hydration, and (iv) Refining the microstructure. Furthermore, over the past few years, the use of nanomaterials has attracted attention in the development of cement concrete. The nanomaterials, including carbon nanotubes (CNTs), nano-SiO_2 (nS), nano-Al_2O_3 (NA), graphene oxide (GO), nano-TiO_2 (NT), nanoclay (NC), nano-ZnO (NZ), and nano-Fe_2O_3 (NF), have proven to provide durability and mechanical performance of concrete [4].

Researchers began incorporating nanomaterials into cement composites, such as nano-silica, which has successfully promoted cement hydration due to its nucleation effect and high specific surface area. However, due to its low aspect ratio, nano-silica tends to slow and even inhibit the formation of microcracks at the nanoscale, thereby leading to poor pore refinement. Thus, nanofibres and nanotubes have been famously used as additives in cementitious composites. However, it also presents a major drawback: these carbon compounds cannot form optimal bonds with cementitious materials due to a lack of interfacial regions between nanoparticles and cementitious materials [8]. As in the incorporation of nano-silica (NS), 4% NS contributes most to compressive strength and is also the highest replacement quantity reported in cement-based materials by past researchers. This is because any usage above the optimal dosage, such as 5%, leads to negative agglomeration effects in the nano-silica particles [9]. Nonetheless, the optimal dosage of nano silica reduces pore diameter by improving pore refinement across the total volume of the microstructure. By all means, they noticed that the total porosity of nanocomposite concrete also decreases, as it creates denser concrete. Not to mention that the usage of nanomaterials also significantly improves the growth of C-S-H, as it provides the nucleation effect.

The same optimal dosage of 4% in the cement matrix can also be achieved by using Nano-titanium dioxide (Nano-TiO_2). It has been reported that the usage of this nanomaterial improved compressive strength by up to 40%. Meanwhile, it has also been reported that the strength of cement mortar with Nano-TiO_2 increased significantly by up to 45% upon the addition of a superplasticiser and slag powder [10]. The addition of a superplasticiser and slag powder improves dispersion and modifies the fluidity of cement mortar. However, the major improvement in strength is solely due to the nucleation effect, which does not involve an increase in the amount of hydration product. In other studies, the optimal dosage of nano-SiO_2 and nano-TiO_2 in the cement matrix was found to be 3% [11]. The study also reported the same findings. Once the dosage reached 5%, compressive strength declined. The strength's downfall was due to agglomeration, and the nanoparticles were prone to gathering in certain spots. Similarly, Nano Iron Oxide (Nano-Fe_2O_3, NF) has been reported to have the smallest effect on the compressive strength of the cement matrix, with a maximum replacement quantity of 3%. In contrast to nano alumina (Al_2O_3, NA), the same optimal replacement of 3% in a cement matrix improves compressive strength by up to 35% [12]. Due to the pozzolanic reaction, it also forms the C-S-H gel, which fills major capillaries in the matrix and eventually reduces the porosity. This also leads to the densification of the cement microstructure and an enhancement in mechanical performance. Another study reported that a 2% addition of nano alumina increased compressive strength by up to 16.36% [11], [13]. However, excessive use of nano alumina can reduce strength due to a reaction with calcium hydroxide, which in turn leads to silica leaching. This could gradually decrease the strength of cement mortar over time.

As reviewed, most research has focused on the influence of nanomaterials on cementitious materials. Nevertheless, graphene has been ignored in the literature. Although still in the early stages of discovery, this carbon-based material has the potential to provide a high-quality enhancement to cement-based materials. Graphene-based nanomaterials can be described as two-dimensional (2D) carbon allotropes composed of sp2-bonded carbon atoms that form a perfect honeycomb lattice [14]. Graphene also exhibits full-stack properties such as ultra-large aspect ratio, thermal stability, surface flexibility, brilliant mechanical properties, gas impermeability, high chemical resistance and high thermal stability. Graphene is also well known for its use as a filler, enhancing the pore refinement of cement paste to its full potential. These characteristics make graphene a promising nanomaterial candidate due to its ability to enhance the performance of conventional materials and provide even greater stiffness to cement-based materials [15]. Although recent literature has shown a clear trend in the effects of slag and fly ash as supplementary cementitious materials, no study has focused on the fresh and

Int. Journal of Integrated Engineering Vol. 18 No. 5 (2026) p. 282-298

mechanical properties of blended cement paste with additional nanomaterials. Therefore, this study intends to extensively fill the above inquiries by providing decent answers to the following questions:

- What percentage of Graphene affects the physical, mechanical and durability properties of cement paste?
- How effective are slag and fly ash as SCM in cementitious material?
- What is the optimum dosage of Graphene and SCMs (slag and fly ash) that maximises the physical, mechanical, and durability properties of cement paste?

To address these questions, several experimental tests were conducted, including a bulk density test and a water absorption test to assess the fresh properties of the cement paste. Compressive, tensile, and flexural tests were performed to determine the impact of SCMs on cement paste, including the nanomaterial Graphene.

2. Material and Experimental Methods

2.1 Raw Materials

In this study, Ordinary Portland Cement (OPC) with CEM I 42.5N was used as the main binder in the mix design, and the chemical compositions of each raw material are also shown in Table 1. Moreover, the fly ash used in the study was obtained from a power plant that produced tonnes of fly ash as waste material over the years. Therefore, the study fully utilised this waste. Meanwhile, the slag was obtained from industrial sectors located in Pahang. The graphene used in this study was produced by graphitisation of petroleum coke waste. It is worth pointing out that graphene can be considered as one of the purest carbon-based materials, whereas Table 2 indicates the reading for the elemental analyser of graphene.

Table 1 *Chemical composition of ordinary Portland cement (OPC), fly ash and slag*

Material	SiO_2 (%)	AI_2O_3 (%)	CaO (%)	Fe_2O_3 (%)	MgO (%)
OPC	19.1	4.97	64.50	3.50	1.87
Fly Ash	59.49	20.0	8.74	4.13	2.94
Slag	35.85	5.08	37.22	7.77	3.55

Table 2 *Elemental analyser data for graphene*

Material	Nitrogen (%)	Carbon (%)	Hydrogen (%)	Sulphur (%)
Graphene	2.70	109.23	9.52	15.41

2.2 Preparation of OPC Cement Paste

The mix design for this study comprised two primary phases: binder formulation and subsequent binder modification. The initial binder formulation phase aimed to determine the optimal replacement percentage of cement with supplementary cementitious materials (SCMs), specifically fly ash and slag, at 10%, 20%, and 30%. Following this optimisation, the binder modification phase focused on identifying the most effective graphene inclusion dosage (0.02%, 0.04%, 0.06%, 0.08% and 0.10%) within the cement paste, utilising the previously established optimal SCM blend.

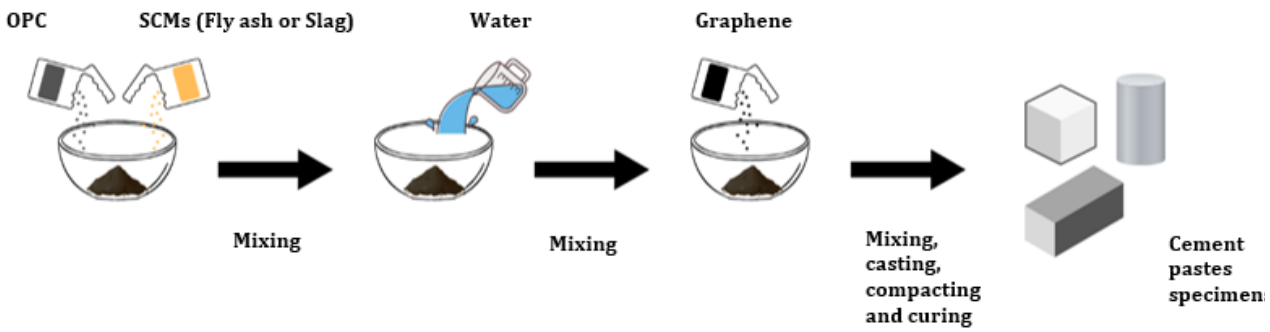


Fig. 1 *Schematic presentation of the manufacturing process for the different types of OPC mortars*

For pure OPC with SCMs cement paste, a water-cement ratio of 0.5 was used in the study. As shown in Fig. 1, the binder formulation began with a design mix comparison between fly ash and slag, which was mixed at high speed for 1 minute, followed by the addition of tap water to the mixer. After mixing, all cement paste samples were poured into different moulds according to their percentages (10%, 20% and 30%) immediately and vibrated on a vibrating table for 30 seconds before curing. Then, all cement paste specimens were cured under identical conditions for 7, 14, and 28 days prior to binder modification. Building on the optimised binder formulation data, this study modifies the binder by incorporating varying percentages of graphene. Table 3 Details the mix proportions of different cement paste specimens used for the initial binder formulation, which included cement replacement levels of 10%, 20%, and 30% with supplementary cementitious materials (SCMs) of fly ash and slag. Further analysis revealed an optimal SCM composition at a specific replacement level (20% fly ash and 30% slag). Subsequently, binder modification was performed using this optimal SCMs blend from the binder formulation, with varying graphene dosages per binder, as presented in Table 4**.** The overall manufacturing process is schematically illustrated in Fig. 1.

Table 3 *Detailed mix proportion of binder formulation*

Mixtures	Cement (%)	Fly Ash (%)	Slag (%)
REF	100.0	-	-
10F	90.00	10.00	-
20F	80.00	20.00	-
30F	70.00	30.00	-
10S	90.00	-	10.00
20S	80.00	-	20.00
30S	70.00	-	30.00

Table 4 *Detailed mix proportion of binder modification (optimal dosage of SCMs achieved)*

Mixtures	Cement (%)	Fly Ash (%)	Slag (%)	Graphene (%)
20FG2	80.00	20.00	-	0.02
20FG4	80.00	20.00	-	0.04
20FG6	80.00	20.00	-	0.06
20FG8	80.00	20.00	-	0.08
20FG1	80.00	20.00	-	0.10
30SG2	70.00	-	30.00	0.02
30SG4	70.00	-	30.00	0.04
30SG6	70.00	-	30.00	0.06
30SG8	70.00	-	30.00	0.08
30SG1	70.00	-	30.00	0.10

2.3 Test Setup and Procedure

2.3.1 Physical Properties Test

The fresh properties of the binder formulation and its modifications were determined by conducting a bulk density test in accordance with ASTM C138.

2.3.2 Mechanical Tests

Three mechanical tests were conducted in the current experiment: compressive strength, flexural strength, and tensile strength. Cubes with dimensions of 50 mm, prisms with dimensions of 40 x 40 x 160 mm, and cylinders with dimensions of 100⌀ x 200 were prepared for the tests. Three repetitions were run to consider the average reading for every test. For the compressive strength test, each dry specimen was loaded in a compression machine at a constant rate of 1.75 kN/s until failure, in accordance with ASTM C109. For the tensile strength test, an axial perpendicular force was applied to the surface of the specimen and split into two. This test was conducted in accordance with the reference standard ASTM C496, up to failure at a rate of 0.7-1.4 MPa/min. Last but not least,

Int. Journal of Integrated Engineering Vol. 18 No. 5 (2026) p. 282-298

for the flexural strength test, three-point loading was adopted and followed the guidelines of ASTM C78. A loading rate of 0.072 mm/min was also used throughout the whole test.

2.3.3 Durability Test

Apparent density, also known as bulk density (ρb), is defined as the ratio of mass to volume of a material, including water and pores. It is also a crucial parameter in material characterisation. Thus, the apparent density test was conducted in accordance with ASTM D1895 (2003).

3. Binder Formulation

Binder formulation can be described as preliminary data that play a crucial role in determining the exact dosage of SCMs required to enhance mechanical strength. This is because the most suitable binder is critical in providing optimal conditions and ensuring the stability of the cement paste. Hence, this study examines the effects of fly ash and slag as blended binders in cement paste formulations. A comprehensive yet concise experimental method was employed with various replacement percentages (10%, 20%, and 30%). The main target was to identify the optimal binder composition to achieve the highest physical and mechanical performance.

3.1 Bulk Density

The graphs in the Fig. 2 represent the bulk density of the binder formulation, which includes the replacement of fly ash and slag in the cement matrix. Moreover, the data collected represent the mean bulk density of samples with replacement percentages of 10%, 20%, and 30%. The bulk density recorded for fly ash is 1.900 g/cm^3, 1.907 g/cm^3 and 1.916 g/cm^3. Meanwhile, the bulk density of slag in cement-blended paste recorded 1.969 g/cm^3, 1.977 g/cm^3, and 1.987 g/cm^3. Technically, both replacement materials showed a similar pattern: bulk density increased linearly with the amount of replacement. However, it has been determined that slag produces a denser blended cement paste than fly ash.

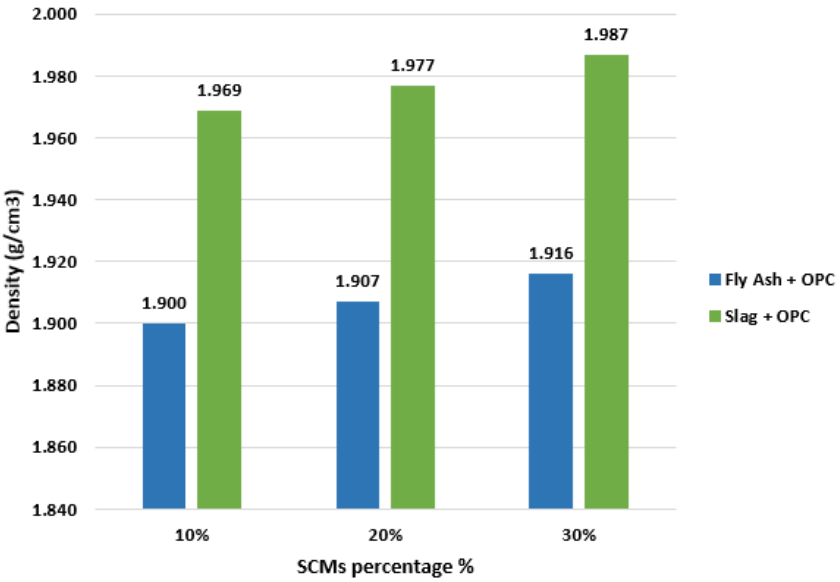


Fig. 2 *Bulk density of binder formulation*

3.2 Compressive Strength

The compressive strength of fly ash and slag as cement replacements in cement paste can be observed at replacement levels of 10%, 20%, and 30%. The data also showed the average compressive strength for both materials at ages 7, 14, and 28 days of curing. Fig. 3 shows that the early compressive strength of the fly ash cement paste was low, starting at 20.43 MPa for 10% replacement, followed by 22.72 MPa and 20.88 MPa for 20% and 30% replacements, respectively. This can be explained by the silica content of fly ash, which enhanced the pozzolanic reaction, leading to C-S-H formation in the concrete after 7 days. Then, the average compressive strength of fly ash replacement began to show an optimal replacement percentage of 20%, with 32.20 MPa after 28 days of curing. Overall, for fly ash cement paste, it is safe to state that 20% fly ash in concrete is sufficient to bind the cement and produce the predicted compressive strength for the study. Similarly, with slag percentage in cement paste, the early strength tends to be low and stagnant at 21.08 MPa, 22.61 MPa, and 20.44 MPa. Nevertheless, the compressive strength increased significantly from mid-strength to late strength. To be more

precise, the 30% replacement in concrete shows the highest compressive strength, 34.60 MPa, followed by the 20% replacement at 34.44 MPa at 28 days of curing. This can be attributed to the presence of Silica (SiO_2), which promotes the pozzolanic reaction with calcium hydroxide during hydration. This contributes to the overall strength of the concrete. On top of that, the difference in the compressive strengths of fly ash- and slag-blended cement paste lies in the Calcium Oxide percentage, with slag having a higher value than fly ash. The presence of calcium oxide in the slag further strengthens the concrete by accelerating the hydration process.

3.3 Tensile Strength

Similarly, with compressive strength data, the tensile strength of fly ash blended cement paste indicated that the strength linearly decreased with the increment of fly ash dosage, as shown in Fig. 4. Not only that, but in the comparison of early strength, the tensile strength values are low across various fly ash percentages. This can be explained by an inconsistent pozzolanic reaction at the fly ash percentage used; therefore, the strength development for each sample differs. Nevertheless, it can be seen that 20% fly ash contributed the highest tensile strength, with values of 2.30 MPa, 3.18 MPa, and 3.50 MPa. Meanwhile, a 30% fly ash content yields the lowest tensile strength. This can be attributed to an excessive amount of fly ash, which causes no significant changes in the sample's strength development and further delays hardening. Moreover, the tensile strength of slag in cement paste shows a slight difference, with the highest values exceeding those of the fly ash-blended cement paste sample. To be more precise, the tensile strength of the 30% slag sample was consistently higher on each curing day than that of the other percentage samples by 2.63 MPa, 3.65 MPa, and 4.01 MPa. The discussion in this matter relates to the previous reason in the compressive strength subtopic, as the amount of Silica (SiO_2) in slag is higher than in fly ash. This shall lead to a greater strength development for the hydration reaction, consequently providing stiffer properties to the sample.

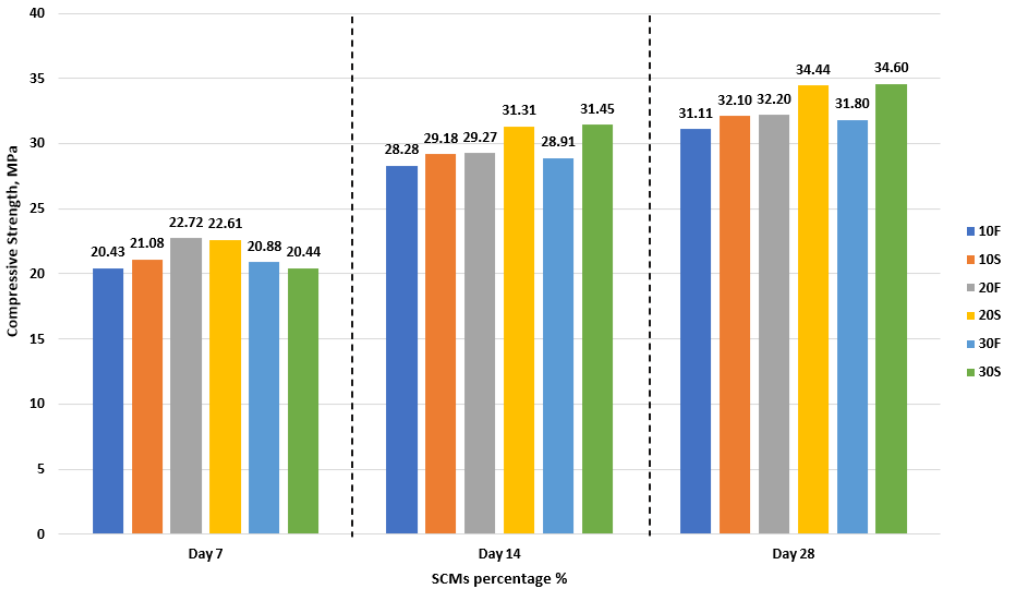


Fig. 3 *Compressive strength of binder formulation*

Int. Journal of Integrated Engineering Vol. 18 No. 5 (2026) p. 282-298

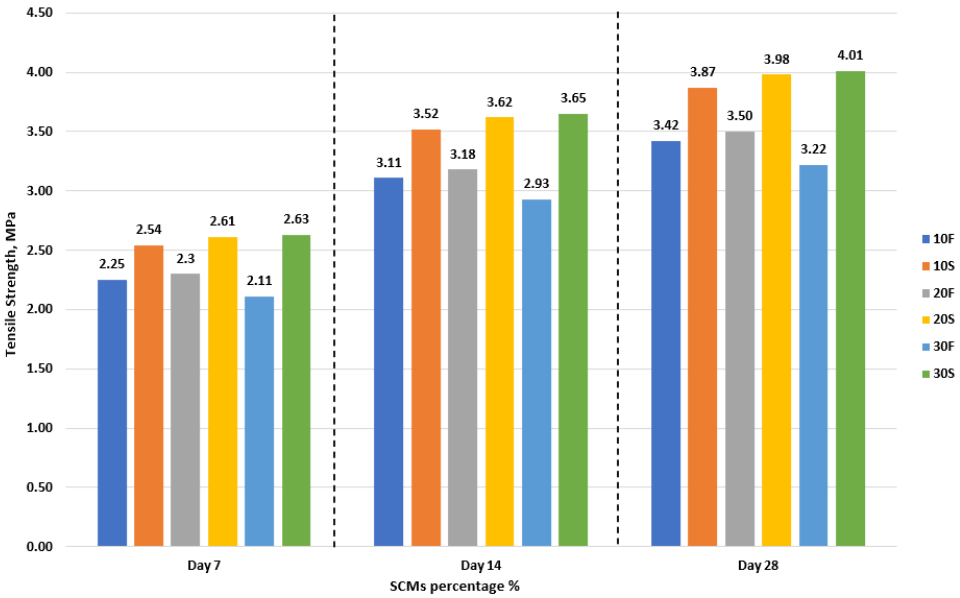


Fig. 4 *Tensile strength of binder formulation*

3.4 Flexural Strength

A similar trend to the previous section, whereby the strength of the cement paste indicated that 20% replacement of fly ash is the optimal dosage needed in the mixture. This can be further analysed in Fig. 5, as a 20% fly ash replacement shows the highest strength value for every day of curing. Over 28 days, 4.22 MPa was the highest value, followed by 3.72 MPa and 3.69 MPa. The result indicated that, for high replacement percentages, the strength of cement paste gradually decreases, indicating no significant benefit of high fly ash usage in the cement matrix. Furthermore, a 30% replacement of cement with slag yields the maximum flexural strength of the cement paste among the replacement percentages. This can be elaborated as the flexural strength gradually increasing with increasing replacement percentage. To be more precise, after 28 days of curing, a compressive strength of 4.65 MPa was achieved with a 30% replacement. Meanwhile, the 20% slag replacement in cement was the second-highest at 4.24 MPa, followed by 3.92 MPa for the 10% replacement. This strongly indicated that slag significantly improved the strength of the cement paste by enhancing the pozzolanic reaction.

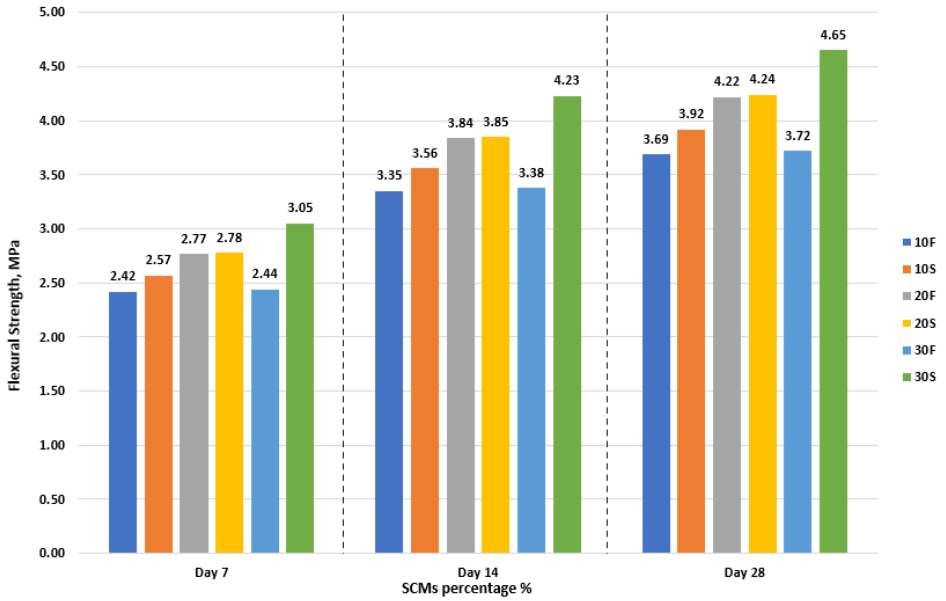


Fig. 5 *Flexural strength of binder formulation*

3.5 Water Absorption

Fig. 6 represents the water absorption for the binder formulation, whereby it consists of SCM material of fly ash and slag with three constant replacement percentages of 10%, 20% and 30%. Overall, the data indicate that the

highest water absorption was recorded at 1.79% with a 10% fly ash replacement, followed by 1.77% with the same replacement. Moreover, the data also shows that water absorption gradually decreases as the replacement percentage increases. This indicates that the replacement material used in the study affects the mixture's porosity and reduces water absorption to some extent. Overall, the results indicate that a 30% slag replacement of cement provides lower water absorption than other samples. This explains how slag acts as an SCM by filling voids in the cement matrix, reducing the pores through which water can penetrate during the water absorption test. In contrast, the lower the SCM replacement percentage, the higher the water absorption.

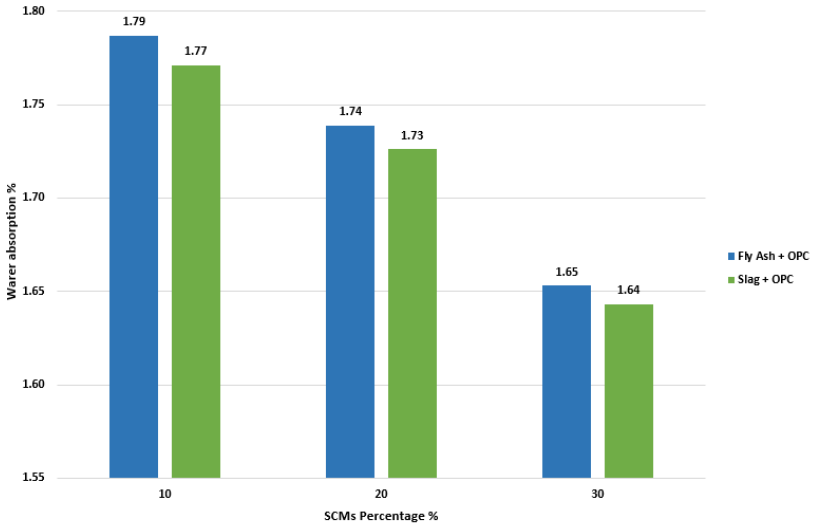


Fig. 6 *Water absorption of binder formulation*

4. Binder Modification

This section discusses the binder modification in the study, which involves incorporating graphene additives into the cement paste. The baseline binder formulation, previously determined through extensive experimental data, was concluded to be 20% fly ash and 30% slag. Hence, various percentages of graphene (0.02%, 0.04%, 0.06%, and 0.08%) were incorporated to study their behaviour and impact on the overall performance of the cement paste. To be more specific, binder formulation data shall maximise the flexibility of graphene as a nanomaterial in cement paste while enhancing the overall sustainability of SCMs as cement replacement in the cement paste.

4.1 Bulk Density

The result shown in Fig. 7 depicts the bulk density of the SCM modification formulation with various graphene replacement contents of 0.02%, 0.04%, 0.06%, 0.08%, and 0.10%. On the overview data, it can be concluded that the average reading for both materials is nuanced or varied. This can be explained by the fact that slag-blended cement paste with graphene tends to yield higher readings than fly ash-incorporated graphene. Nevertheless, the increase in density observed in slag-blended cement paste with 0.02% graphene can be attributed to graphene itself, which tends to promote the filling effect. With an adequate amount of graphene, it conceals microcrack formation and restricts further crack development due to substantial bonding with the cement matrix. On top of that, a reduction in density can also be described as the possibility of agglomeration, which consequently leads to a non-homogeneous mixture.

Int. Journal of Integrated Engineering Vol. 18 No. 5 (2026) p. 282-298

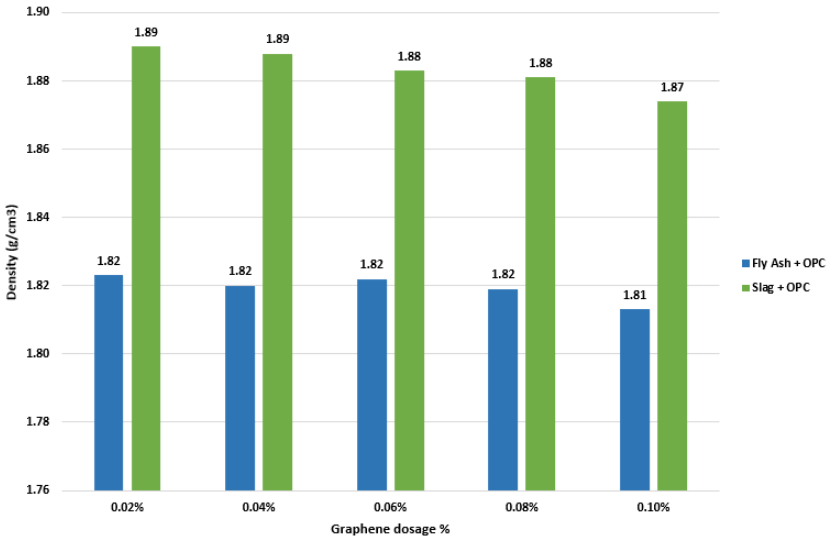


Fig. 7 *Bulk density of binder modification*

4.2 Compressive Strength

The average compressive strength of binder modification can be presented in Fig. 8. It can be observed that in the early days of strength development, the range of strength obtained is between 22.85 MPa and 21.67 MPa. Technically, the compressive strength of each sample varied with the inclusion of graphene of 0.02%, 0.04%, 0.06%, 0.08% and 0.10%. Moreover, at 28 days, the compressive strength tends to show the predicted strength of mature cement paste. The inclusion of 0.02% graphene in fly ash-blended cement paste achieved the highest compressive strength among the graphene contents, at 34.80 MPa. This compressive strength could be optimised by considering the ideal fly ash content with peak graphene percentage. This can be explained by the pozzolanic activity, which tends to accelerate at high reaction rates in the mixture. Not only that, but with the help of graphene, it features the mechanism of the filling effect, whereby it reduces porosity, which consequently increases the strength of the sample. Incorporating graphene into the mixture also increases compressive strength by enhancing the hydration mechanism, thereby promoting strength development. However, as the graphene content in the sample increases, the compressive strength tends to decline. This might occur due to graphene's low dispersion, which not only reduces strength but also increases the potential for agglomeration.

As for slag in binder modification, Fig. 8 also shows that the compressive strength of the tested specimens ranged from 21.67 MPa to 23.35 MPa, 30.01 MPa to 32.34 MPa, and 33.01 MPa to 35.57 MPa at 7, 14, and 28 days, respectively. However, better results were achieved with a 0.02% graphene combination, which yielded the highest compressive strength of 35.57 MPa. This can be described as graphene, famously known for its monolayer and few-layer forms, with a large specific surface area. Not only that, but it also consists of a high value of Young's modulus (2TPa). Graphene tends to provide strong interactions during cement hydration, which indirectly helps form the major components of C-S-H [14]. This can be explained by graphene having one of the largest surface areas among nanomaterials. This creates beneficial traits in graphene that enhance its chemical reaction with the cement matrix, especially during the strength development stage. More specifically, for a faster, more effective chemical reaction, the nanomaterial's surface area is essential. Therefore, graphene can react rapidly with hydration products, such as Calcium Hydroxide, to form C-S-H gel. Moreover, the growth of efficient C-S-H tends to provide a denser microstructure and even micropores within any transition area of the cement matrix, which are filled perfectly. Hence, this leads to a higher-quality mixture with greater strength capacity. Moreover, the high surface area of graphene helps C-S-H particles bond well with graphene, which acts as a nucleation site, continuously promoting C-S-H growth along the graphene flakes. This ultimately leads to an increment in strength in the bond strength of the cement matrix. This eventually results in greater stiffness within the sample, thereby increasing the load-transfer efficiency from the cement matrix to the reinforcement. This can also be related to the "bridging effect" in graphene, whereby its hydrophilic nature significantly enhances interlayer interactions within the cement matrix. This shall lead to a greater load-bearing capacity enhancement for the mixture when loads are being applied.

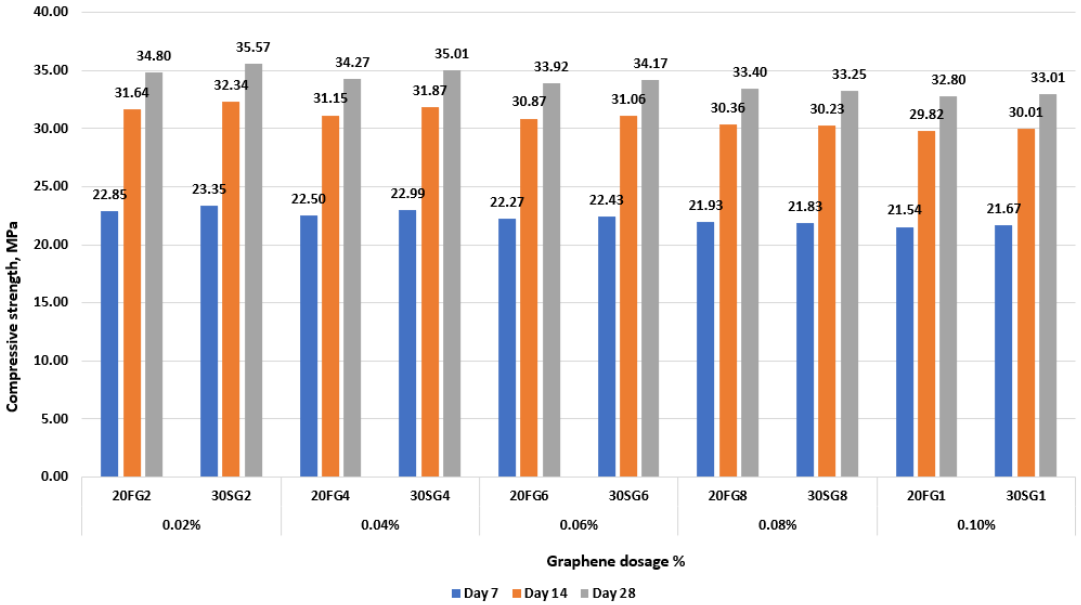


Fig. 8 *Compressive strength of binder modification*

Fig. 9 depicts the increment in compressive strength for each percentage of graphene in the cement paste sample. While a noticeable increase in compressive strength was observed at 7 days of curing, the effect of graphene on strength was more pronounced at 28 days. The previous discussion identified 0.02% graphene as the optimal percentage in the cement paste for both SCM samples. To be more precise, 30SG2 has the highest compressive strength, increasing by 20.74%. Moreover, 20FG2 achieved a 20.72% increase in compressive strength. Nevertheless, 30SG2 is still nominated as having the highest compressive strength in the overall observation of the binder modification results. This can be discussed by noting that graphene has high tensile strength, which enhances bridging of microcracks within the cement matrix, thereby preventing crack propagation.

4.3 Tensile Strength

Fig. 10 depicts the tensile strength of all experimental samples with different curing days and various graphene contents. The initial observation showed a 7.67% difference between the highest and lowest readings. In detail, the inclusion of 0.02% graphene as a fly ash cement replacement in cement paste resulted in tensile strengths of 2.30 MPa, 3.19 MPa, and 3.51 MPa at 7, 14, and 28 days, respectively. The increase in strength can be attributed to the partial substitution of fly ash with graphene, which promotes faster hydration during hardening. This contributes to one of the major references of graphene as a nucleation effect towards the cement composite mechanism. Nevertheless, the data analysis continues, as the strength decreases moderately when graphene is added to the mixture. This might happen due to a lack of homogenous dispersion in the mixture, leading to lower load capacity in the sample. Moreover, this figure also describes the tensile strength of slag-blended cement paste with graphene. The tensile strength of slag incorporated with graphene ranges from 1.98 MPa to 2.75 MPa, 2.74 MPa to 3.81 MPa, and 3.01 MPa to 4.19 MPa at 7, 14, and 28 days, respectively.

Int. Journal of Integrated Engineering Vol. 18 No. 5 (2026) p. 282-298

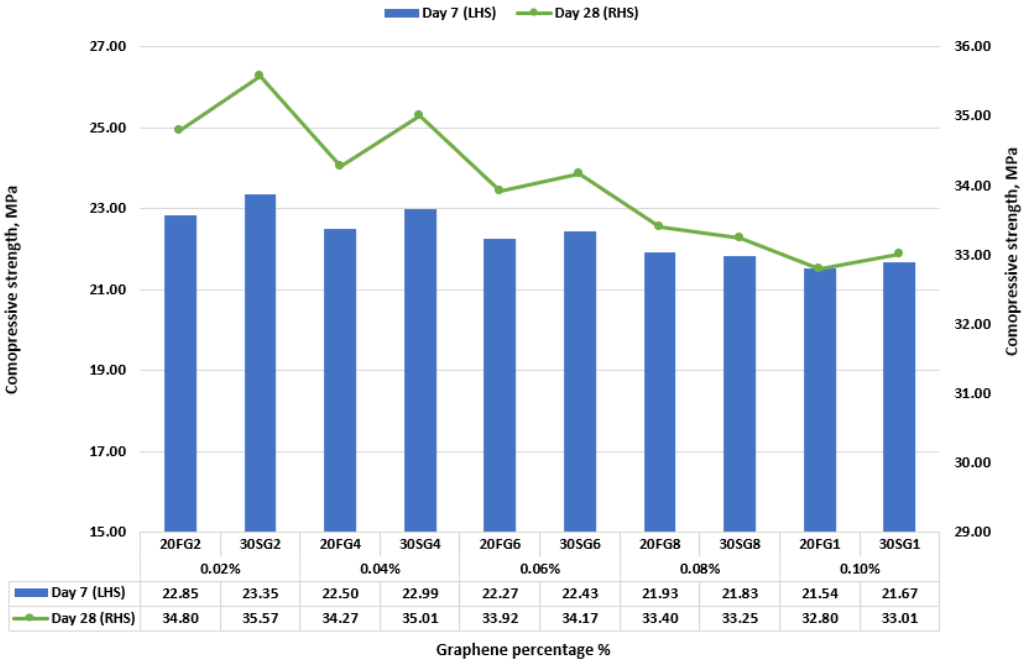


Fig. 9 *Combination graph of increment compressive strength of binder modification*

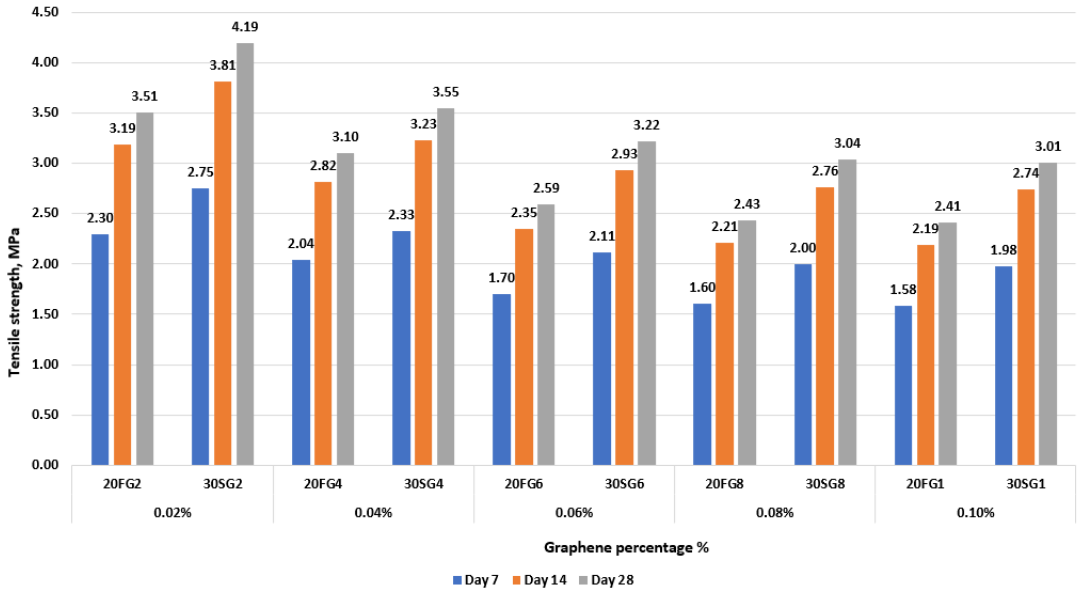


Fig. 10 *Tensile strength of binder modification*

Similar to the previous parameter, compressive strength, 0.02% graphene performed exceptionally well with slag, yielding the highest tensile strength among the mixture samples. To be exact, the strength increment for 0.02% graphene was 16.39% after 28 days. Carbon-based materials, such as graphene, continue to provide a sheet-like microstructural configuration that helps prevent cracks under load [16]. In addition, graphene also contributes towards the densification of the sample due to the filling effect. The filling effect can be explained by the tendency of nanosized graphene particles to interlock and fill available pores in the sample. Consequently, it yields a denser sample than others. Fig. 11 shows a combined graph that clearly indicates the significant increase in SCMs-blended cement paste at 7 and 28 days of curing. Overall, the data show an increase for each sample. To be more precise, 30SG2 achieved 4.19 MPa after 28 days of curing, representing a 20.75% increase. However, a clear downward trend was observed, indicating that as the graphene percentage increases, tensile strength decreases. For example, 30SG1 showed a 1.98 MPa reduction in tensile strength compared to 30SG2. This can be explained as the accumulation of graphene in the cement matrix, which consequently leads to agglomeration of the product.

4.4 Flexural Strength

Fig. 12 shows the flexural strength of fly ash-blended cement paste with graphene added at different percentages. Overall, the observed optimum flexural strength is noted at 7.94 MPa, 11.21 MPa, and 12.10 MPa at 0.02% graphene, while the minimum flexural strength is recorded at 4.85 MPa, 6.72 MPa, and 7.39 MPa at 0.10% graphene as a nanomaterial after 7, 14, and 28 days, respectively. From this figure, it is evident that the use of graphene as a nanomaterial in the cement matrix warrants attention, due to the nano-sized particles of graphene, which clearly fill the pores left by other constituents of the mixture. This leads to a more extensive interlocking mechanism that involves both physical and mechanical bonding [17]. In addition to the existing benefits of fly ash, it also boosts the pozzolanic activity in the mixture during hydration, leading to stronger bond development. Similarly, the flexural strength of slag-blended cement paste is significantly higher when 0.02% graphene is used as an additional nanomaterial. The maximum flexural strength for 28 days of curing is recorded by 13.37 MPa, 12.49 MPa, 11.24 MPa, 8.34 MPa and 7.17 MPa at 0.02%, 0.04%, 0.06%, 0.08% and 0.10% of graphene as a nanomaterial in the mixtures.

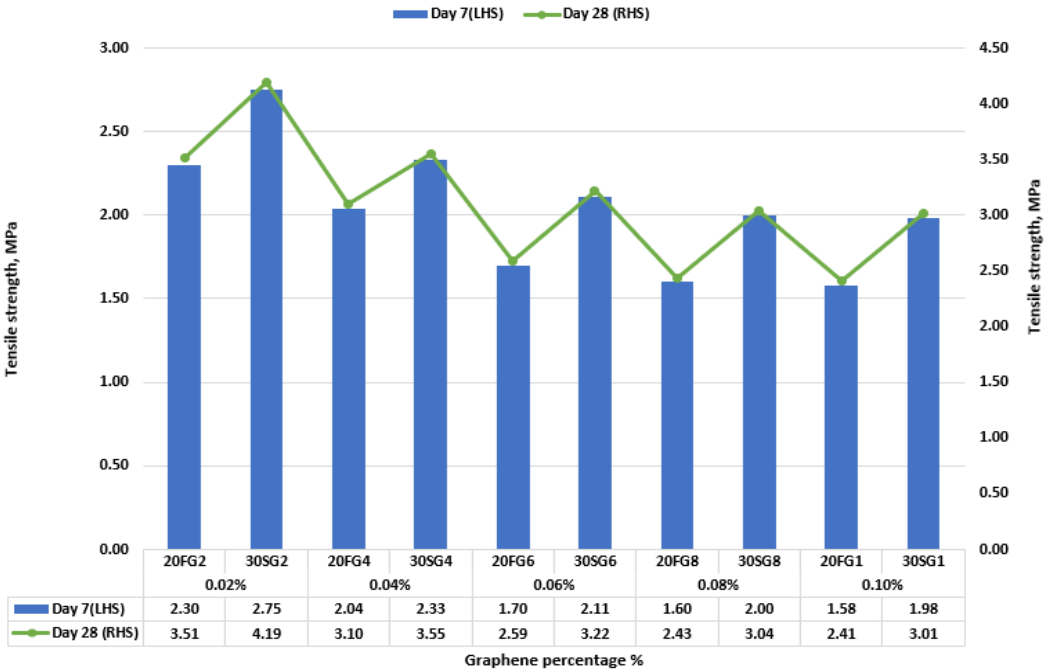


Fig. 11 *Combination graph of the increment in tensile strength of binder modification*

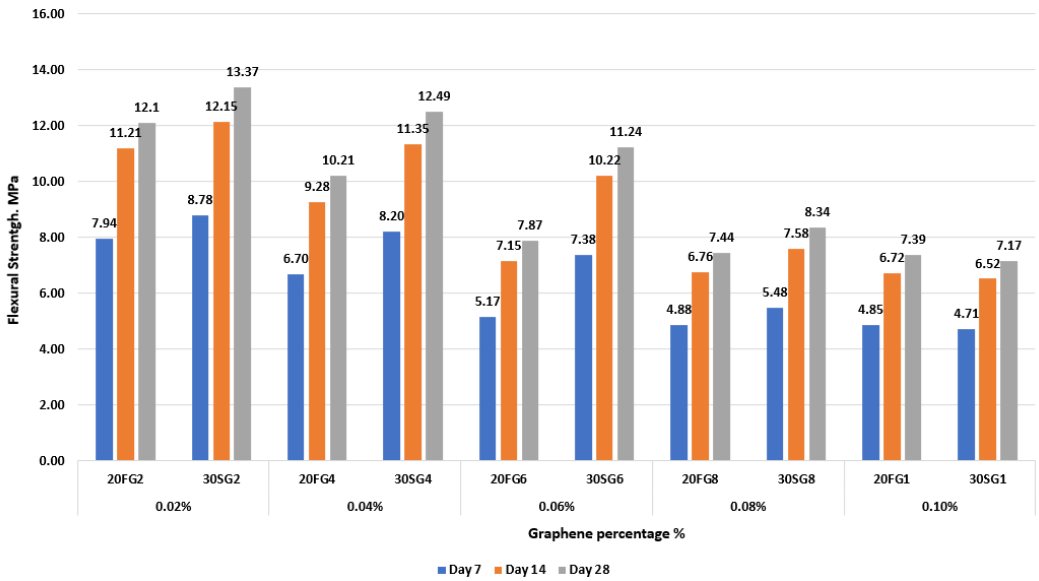


Fig. 12 *Flexural strength of binder modification*

Int. Journal of Integrated Engineering Vol. 18 No. 5 (2026) p. 282-298

Nonetheless, the high amount of Silica in slag contributes towards higher pozzolanic characteristics in the mixture. On the contrary, the lowest recorded flexural strength is 7.17 MPa at 0.10% graphene as a nanomaterial. The reduction in strength can be explained by the high tendency of graphene agglomeration after 0.02% addition. This leads to the non-uniform distribution of graphene in the cement matrix. It is also devoted to the issue of low bearing capacity, as many voids remain unfilled by the graphene. Therefore, the overall strength could be affected at this point and forward. The data presented in Fig. 13 provide valuable insights into the incremental changes in the flexural strength of binder modification at 7 and 28 days of curing. Firstly, it can be stated that 0.02% graphene significantly influenced the flexural strength, as it exhibited the maximum strength among the percentages. A striking feature of this data is that 20FG2 and 30SG2 obtained overall flexural strengths of 12.1 MPa and 13.37 MPa, respectively, in the study. The difference between these two data points is considerable, with a slight 4.98% difference in flexural strength. In addition, the data show an increase from day 7 to 28 days of curing, indicating that graphene, as a nanomaterial, is effective in the cement matrix at an adequate percentage.

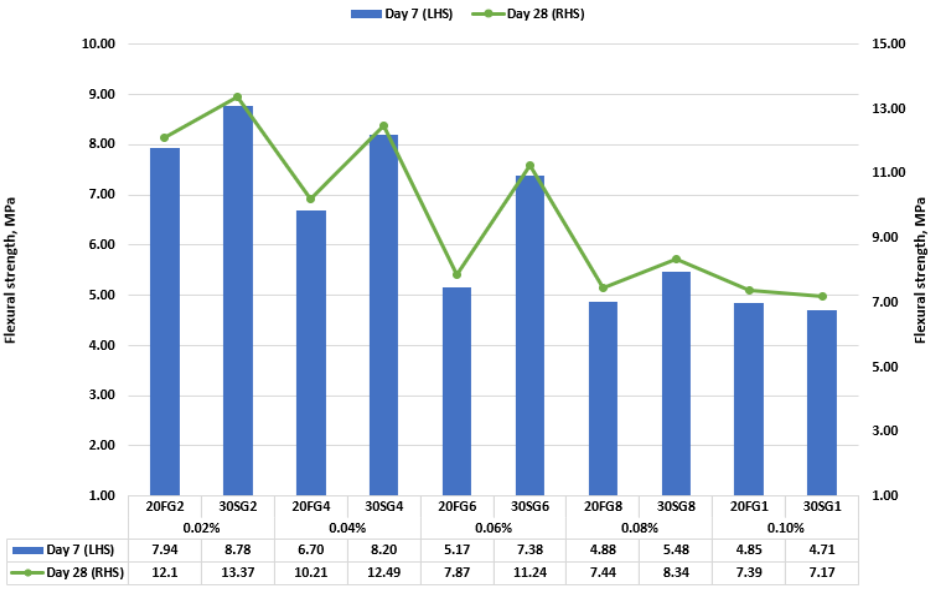


Fig. 13 *Combination graph of increment flexural strength of binder modification*

Henceforth, Table 5 provides a comprehensive yet concise summary of all the mechanical properties data presented in the paper. This table also allows an overall observation of each data obtained precisely with the aid of an informational discussion.

Table 5 *Summary of mechanical properties data*

Mechanical Properties	Overall summary
Compressive strength	• As an overall summary, it can be stated that both of the SCMs' materials used as cement replacements in this study managed to enhance the mechanical properties of the cement paste. This can be shown: Fly ash and slag cement paste delivered a favourable yet enhanced compressive strength, up to 30 MPa, as a reference compressive value in the binder formulation. This can be explained by the chemical composition of fly ash, which effectively facilitates cement hydration by providing sufficient silica. This shall enhance the hydration product as a pozzolanic reaction occurs in the cement paste. Meanwhile, slag tends to provide a higher amount of calcium, which differentiates the compressive strength of fly ash and slag samples. • Nevertheless, it is also worth stating that with the inclusion of graphene in binder modification, the compressive strength of both SCMs increased greatly. With the aid of graphene, a filling-effect mechanism in the cement matrix is observed, resulting in denser cement paste and lower porosity. Therefore, it is evident that 0.02% graphene enhanced the potential of both SCMs in the study. In terms of compressive strength, 30SG2 achieved a greater compressive strength than fly ash-blended cement paste 20FG2, at 35.57 MPa and 34.80 MPa, respectively.

Mechanical Properties	Overall summary
Tensile strength	• As for the tensile strength, the binder formulation tends to provide a similar optimal percentage of SCMs for the cement paste, as 20% of fly ash and 30% of slag. However, it can also be concluded that slag cement paste exhibits higher tensile strength than fly ash cement paste. • For the binder modification, it is crystal clear that 0.02% of graphene still managed to be devoted as the most optimal percentage of graphene in the cement matrix. This can be explained by 20FG2 and 30SG2 achieving the highest tensile strength among the graphene percentages. This can be explained by graphene's tendency to provide a sheet-like microstructural configuration, which can prevent crack formation in the cement matrix, especially under applied loads. However, 30GS2 has the highest tensile strength, at 4.19 MPa, compared to 20FG2 in the study.
Flexural strength	• Similarly, with previous discussions on binder formulation, 20% of fly ash and 30% of slag still managed to become the most optimal SCMs percentage replacement in the cement paste. • The tensile strength shown for the binder modification also indicated that 0.02% of graphene was the optimum dosage in the cement paste, as it shows the highest tensile strength for both SCMs. To be more precise, the tensile strength of 20FG2 was 12.1 MPa, while 30SG2 was 13.37 MPa. This can be justified by the fact that the addition of graphene provided a strong interlocking mechanism within the cement matrix, resulting in high-quality bonding during cement hydration. However, in every set of mechanical properties data, any graphene percentage greater than 0.02% is associated with a reduction in strength. This might have happened due to agglomeration in the cement matrix caused by non-uniform distribution, which eventually leads to high porosity and potential crack formation.

4.5 Water Absorption

Fig. 14 depicts the water absorption of binder-modification samples incorporating graphene at various percentages. It can be observed that the lowest water absorption for both blended cement pastes occurs at 0.02% graphene. As for the fly ash blended sample, the reading indicates 1.49% water absorption. Meanwhile, the slag blended sample shows 1.47%. Moreover, the highest water absorption occurred at 0.10% graphene, at 2.23% for the slag-blended sample and 2.06% for the fly ash-blended sample. The data can be analysed to visualise the effectiveness of graphene at 0.02% as a nanomaterial. On top of that, it indicated that graphene itself tends to significantly enhance the filling effect in the samples. Nevertheless, as the amount of graphene in the sample increases, the water absorption tends to show a higher water absorption reading, meaning that the formation of agglomeration might happen along the way. This eventually leads to a non-homogeneous mixture in the sample, resulting in higher void content and allowing more water to infiltrate it.

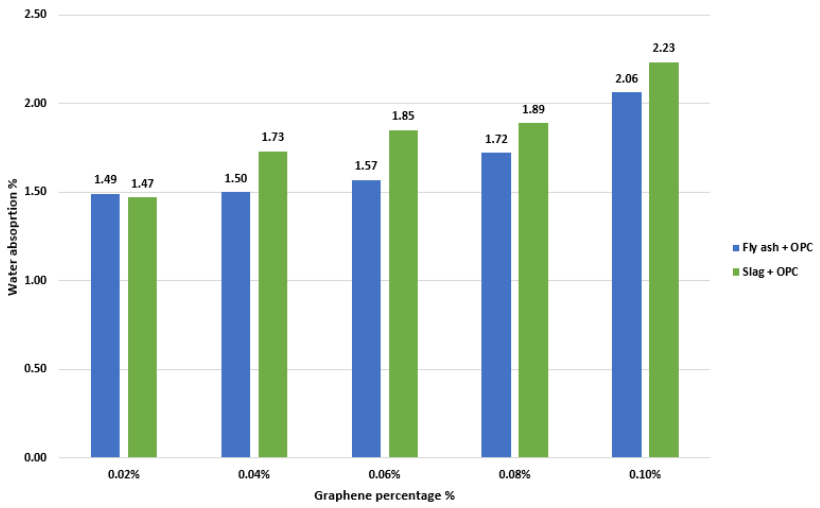


Fig. 14 *Water absorption of binder modification*

Int. Journal of Integrated Engineering Vol. 18 No. 5 (2026) p. 282-298

5. Conclusion

This study presents a comprehensive analysis of the currently prominent nanomaterial, graphene, in cementitious matrix materials. Notably, graphene is an exceptional material that delivers significant performance as a filler agent, promotes gel pore development, refines pores, and improves compositional strength in cement. The large specific area contributes to the astonishing performance of the modified cement composite. Moreover, these factors facilitate improved cement hydration, gel pore formation, and consistent pore distribution, thereby enhancing the structural strength of the cement composite. In addition, graphene increased the durability of the cement composite by acting as a water barrier, thereby providing greater resistance to chemical penetration. In terms of environmental impact, graphene cement composite significantly reduces carbon dioxide emissions. The inclusion of graphene in the cement matrix also enhances performance in densification, microcrack bridging, strength, and even the prevention of microcrack formation. However, graphene agglomeration and workability remain a challenge in forming well-strengthened cementitious composite concrete. Although graphene is well dispersed in water, achieving a uniform dispersion in the cement matrix remains a challenge that warrants further study. Thus, the optimal dosage of graphene is crucial, as it may ensure consistency in cement, which affects the overall performance of the cement composite. Therefore, extensive research on graphene in cement composites is needed to overcome the limitations of its use. On top of that, it can fully maximise the utilisation of graphene composites, making it an encouraging construction material for industry in the future. Moreover, as seen in the research tests being conducted, various results were obtained for certain tests. The critical findings of the present study are as follows:

- The binder formulation shows that the optimal percentages of slag and fly ash as a supplementary cementitious material in the cement matrix were 20% and 30%.
- As in the overall view results of cement paste properties in binder formulation, it can be concluded that 30% of slag (30S) shows greater results than 20% of fly ash (20F). This can be proven, as slag tends to produce denser blended cement paste than fly ash. This also explains the mechanical properties of the cement paste, as a 30% slag replacement in the cement matrix yielded the highest compressive strength, owing to the presence of Silica (SiO_2), which contributed to the pozzolanic reaction with calcium hydroxide during hydration. Nevertheless, it can also be said that 20% of fly ash remains an optimal value.
- As for the physical properties of the binder formulation, 30% of slag has been proven denser compared to other percentages, followed by 30% of fly ash. Moreover, regarding mechanical properties, the binder formulation results continue with compressive strength, showing that 30S achieved the highest value of 34.60 MPa after 28 days of curing. Meanwhile, the second-highest compressive strength was dominated by 20F by 34.44 MPa. In addition, the binder formulation showed 30G as the highest tensile strength, at 4.01 MPa, followed by 20F at 3.98 MPa. Finally, the maximum flexural strength of 4.65 MPa was observed in 30S, while 4.24 MPa was recorded for 20F. The durability properties of the binder formulation led to the conclusion that the higher the SCMs percentages, the lower the water absorption. This can be shown by 30% slag, which achieved the lowest water absorption.
- For the binder modification, it can be proven that 0.02% of graphene influenced the enhancement of both SCM replacements (20FG2 and 30SG2) in the cement matrix. This can be shown in the physical properties of binder modification, with the inclusion of 0.02% graphene, which has significantly increased the density of cement paste for 30SG2 and 20FG2 to 1.82 g/cm3 and 1.89 g/cm3. This shall explain the role of graphene in restricting crack formation in the cement matrix, thereby providing denser cement paste. Moreover, for the compressive strength of binder modification, the results showed a significant value of 35.57 MPa, with the second-highest value of 34.80 MPa for 30G2 and 20FG2. This can be explained by graphene's ability to provide an interlocking mechanism within the cement matrix, thereby enhancing the bonding strength of the cement paste. Moreover, the reduction in strength in binder modification is often due to graphene agglomeration, which typically occurs when more than 0.02% graphene is added. The results indicate a tensile strength, with a similar result observed for 0.02% graphene, demonstrating the effectiveness of cement paste. The highest tensile strength was 4.19 MPa, obtained by 30SG2, followed by 3.51 MPa for 20FG2. This marks the use of graphene as a nanomaterial, thereby enhancing the strength of the cement paste. The maximum flexural strength recorded with slag replacement was 13.37 MPa for 30SG2, while the minimum was 7.17 MPa. Moreover, fly ash replacement showed the same trend, with 0.02% graphene yielding the highest flexural strength of 7.94 MPa. Nevertheless, 30SG2 achieved the maximum overall flexural strength in the binder modification, indicating the effectiveness of slag as a replacement material and graphene as an additive nanomaterial. As in the water absorption test, concurrently, the lower the graphene percentages used, the lower the water absorption recorded. This shows how efficient 30SG2 and 20FG2 are in this test, with 1.47% and 1.49% recorded as the lowest water absorption percentages.
- An adequate amount of graphene features a brilliant mechanism of filling effect, where it helps to reduce the porosity in the cement matrix, producing greater stiffness properties of the sample.

- Graphene also helps facilitate the hydration mechanism in the cement matrix during cement hydration, which leads to improvement in the properties of the cement paste.
- The addition of graphene to the cement matrix also produced a "bridging effect" where it significantly empowered the interaction between layers of the cement matrix material.

Acknowledgement

The authors would like to thank the Faculty of Civil Engineering, Universiti Teknologi MARA (UiTM) Shah Alam, for their support.

Conflict of Interest

The authors declare no conflicts of interest regarding the publication of this paper.

Author Contribution

The authors confirm contribution to the paper as follows: study conception and design: ***Nazirah Mohd Apandi, Warid Wazien Ahmad Zailani****; data collection:* ***Khairul Nazhan Khairul Izwan, Alia Sofea Shamsol****; analysis and interpretation of results:* ***Khairul Nazhan Khairul Izwan, Nazirah Mohd Apandi, Warid Wazien Ahmad Zailani, Alia Sofea Shamsol****; draft manuscript preparation:* ***Khairul Nazhan Khairul Izwan, Nazirah Mohd Apandi****. All authors reviewed the results and approved the final version of the manuscript.*

References

[1] Zhang, T., Gao, P., Gao, P., Wei, J., & Yu, Q. (2013). Effectiveness of novel and traditional methods to incorporate industrial wastes in cementitious materials—An overview. Resources, Conservation and Recycling, 74, 134–143. https://doi.org/10.1016/j.resconrec.2013.03.003

[2] Ganesh, S., Thambiliyagodage, C., Perera, S. V. T. J., & Rajapakse, R. K. N. D. (2023). Influence of laboratory synthesized graphene oxide on the morphology and properties of cement mortar. Nanomaterials, 13, 18. https://doi.org/10.3390/nano13010018

[3] Anwar, A., Mohammed, B. S., Wahab, M. A., & Liew, M. S. (2020). Enhanced properties of cementitious composite tailored with graphene oxide nanomaterial - A review. Developments in the Built Environment, 1, 100002. https://doi.org/10.1016/j.dibe.2019.100002

[4] Abdalla, J. A., Thomas, B. S., Hawileh, R. A., & Syed Ahmed Kabeer, K. I. (2022). Influence of nanomaterials on the workability and compressive strength of cement-based concrete. Materials Today: Proceedings, 65, 2073–2076. https://doi.org/10.1016/j.matpr.2022.06.429

[5] Apandi, N. M., Ma, C.-K., Chin, C.-L., Awang, A. Z., & Wazien, W. (2023). Stress strain response of pre-damaged concrete confined with recycled steel straps—A green confining material. Journal of Building Engineering, 75, 106760. https://doi.org/10.1016/j.jobe.2023.106760

[6] Ma, C.-K., Chin Siew Yung, S., Apandi, N., Zawawi Awang, A., & Omar, W. (2017). Innovative concrete repairing technique using post tensioning steel straps. MATEC Web of Conferences, 103, 02011. https://doi.org/10.1051/matecconf/201710302011

[7] Vantadori, S., Magnani, G., Mantovani, L., Pontiroli, D., Ronchei, C., Scorza, D., Sidoli, M., Zanichelli, A., & Riccò, M. (2022). Effect of GO nanosheets on microstructure, mechanical and fracture properties of cement composites. Construction and Building Materials, 361, 129368. https://doi.org/10.1016/j.conbuildmat.2022.129368

[8] Rafiee, M. A., Lu, W., Thomas, A. V., Zandiatashbar, A., Rafiee, J., Tour, J. M., & Koratkar, N. A. (2010). Graphene nanoribbon composites. ACS Nano, 4, 7415–7420. https://doi.org/10.1021/nn102529n

[9] Zhao, L., Guo, X., Liu, Y., Ge, C., Guo, L., Shu, X., & Liu, J. (2017). Synergistic effects of silica nanoparticles/polycarboxylate superplasticizer modified graphene oxide on mechanical behavior and hydration process of cement composites. RSC Advances, 7, 16688–16702. https://doi.org/10.1039/C7RA01716B

[10] Son, D.-H., Hwangbo, D., Suh, H., Bae, B.-I., Bae, S., & Choi, C.-S. (2023). Mechanical properties of mortar and concrete incorporated with concentrated graphene oxide, functionalized carbon nanotube, nano silica hybrid aqueous solution. Case Studies in Construction Materials, 18, e01603. https://doi.org/10.1016/j.cscm.2022.e01603

[11] Meng, T., Yu, Y., Qian, X., Zhan, S., & Qian, K. (2012). Effect of nano-TiO_2 on the mechanical properties of cement mortar. Construction and Building Materials, 29, 241–245. https://doi.org/10.1016/j.conbuildmat.2011.10.047

[12] Ren, J., Luo, X., Bai, R., Pan, C., & Zhang, J. (2022). Pore characteristics of different phase in nano-modified concrete and their influences on compressive strength. Journal of Building Engineering, 46, 103784. https://doi.org/10.1016/j.jobe.2021.103784

[13] Kantharia, M., & Mishra, P. K. (2021). Investigation on compressive strength of cement mortar with nano alumina. Materials Today: Proceedings, 47, 7181–7183. https://doi.org/10.1016/j.matpr.2021.06.410

[14] Anwar, A., Liu, X., & Zhang, L. (2023). Nano-cementitious composites modified with graphene oxide—A review. Thin-Walled Structures, 183, 110326. https://doi.org/10.1016/j.tws.2022.110326

[15] Zhang, R., Yu, X., Yang, Q., Cui, G., & Li, Z. (2021). The role of graphene in anti-corrosion coatings: A review. Construction and Building Materials, 294, 123613. https://doi.org/10.1016/j.conbuildmat.2021.123613

[16] Khed, V. C., Pesaralanka, V., Adamu, M., Ibrahim, Y. E., Azab, M., Reddy, M. A. K., Hakamy, A., & Deifalla, A. F. (2022). Optimization of graphene oxide incorporated in fly ash-based self-compacting concrete. Buildings, 12, 2002. https://doi.org/10.3390/buildings12112002

[17] Mohammed, A., Sanjayan, J. G., Nazari, A., & Al-Saadi, N. T. K. (2018). The role of graphene oxide in limited long-term carbonation of cement-based matrix. Construction and Building Materials, 168, 858–866. https://doi.org/10.1016/j.conbuildmat.2018.02.082